#### **ORIGINAL ARTICLE**



# Investigating the influence of trichostatin A on gene expression modulation associated with parthenolide biosynthesis and accumulation in *Tanacetum parthenium* (feverfew)

Maryam Alimirzaee¹ · Ahmad Moieni² □ · Mohammad Reza Abdollahi³,4 · Dara Dastan⁵

Received: 24 May 2024 / Accepted: 29 August 2024 / Published online: 27 September 2024 © The Author(s), under exclusive licence to Springer Nature B.V. 2024

#### **Abstract**

Tanacetum parthenium, commonly known as feverfew, is a perennial medicinal herb renowned for its therapeutic properties, particularly attributed to the sesquiterpene lactone parthenolide. This study explores the regulatory impact of Trichostatin A (TSA), an epigenetic modulator, on the expression of genes associated with parthenolide biosynthesis and accumulation in *T. parthenium*. We assessed the expression profiles of key genes, namely Germacrene A synthase (GAS), Parthenolide synthase (PTS), and Hydroxy-2-methyl-2-(E)-butenyl 4-diphosphate reductase (HDR) with qRT-PCR. The experimental approach involved treating feverfew plants with varying concentrations of TSA through seed pretreatment under in vitro conditions and foliar spray on in vivo-cultured plants. Our findings indicate that specific concentrations of TSA, notably 0.5  $\mu$ M and 1  $\mu$ M, positively modulate the expression of GAS and PTS genes, thereby influencing the final concentration of parthenolide. This research provides valuable insights into the potential of TSA as a strategic tool for enhancing secondary metabolite production in medicinal plants.

#### Key message

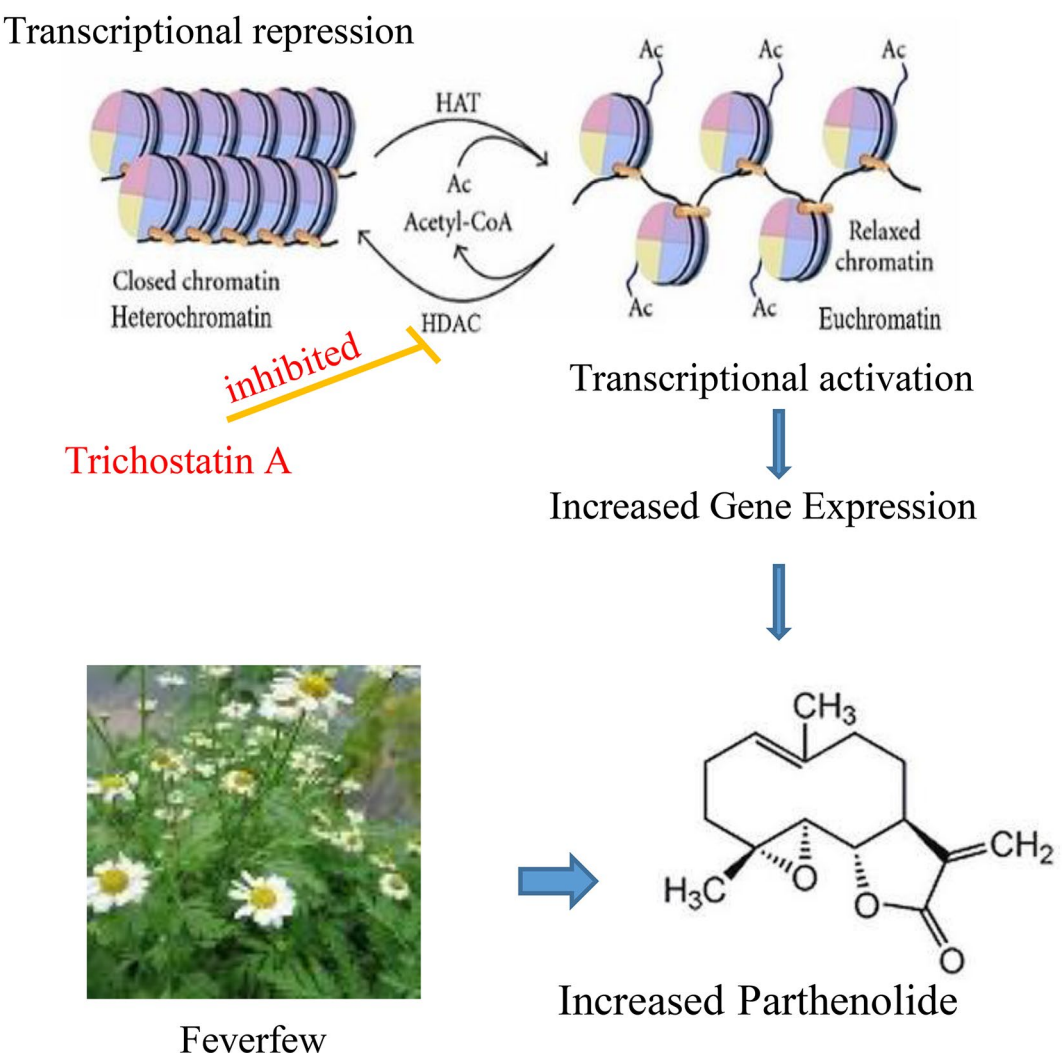
Trichostatin A (TSA), a typical histone deacetylase inhibitor, can increase the production of parthenolide (a major sesquiterpene lactone) in the in vivo plants and *in vtiro* seedlings of feverfew.

#### Communicated by Sergio J. Ochatt.

- Ahmad Moieni moieni\_a@modares.ac.ir
- Mohammad Reza Abdollahi m.abdollahi@basu.ac.ir
- Department of Agricultural Biotechnology, Tarbiat Modares University, Tehran, Iran
- Department of Plant Genetics and Breeding, Tarbiat Modares University, Tehran, Iran
- Department of Plant Production and Genetics, Faculty of Agriculture, Bu-Ali Sina University, Hamedan, Iran
- <sup>4</sup> Plant Chemistry Research Center, Bu-Ali Sina University, Hamedan, Iran
- Department of Pharmacognosy, Medicinal Plants and Natural Products Research Center, Hamadan University of Medical Sciences, Hamadan, Iran



# **Graphical Abstract**



Keywords Epigenetic modulator · Secondary metabolite · Histone acetylation · Relative gene expression

#### **Abbreviations**

GAS	Germacrene A synthase
GAO	Germacrene A oxidase
COS	Costunolide synthase
PTS	Parthenolide synthase
HDR	Hydroxy-2-methyl-2-(E)-butenyl 4-diphos-
	phate reductase
TSA	Trichostatin A
IDP	Isopentenyl diphosphate
DMADP	Dimethylallyl diphosphate
MVA	Mevalonic acid
MEP	Methylerythritol phosphate
<b>HDACs</b>	Histone deacetylases

Histone acetyltransferases

# Introduction

Feverfew (*Tanacetum parthenium* L.) Bip.), a member of the Asteraceae family, is a medicinal herb with a long history of traditional use for various diseases, including toothache, stomachache, migraine, fever, arthritis, and helminthiasis (Simmons et al. 2002). Feverfew contains many sesquiterpene lactones, of which parthenolide is the highest concentration (up to 85%) of sesquiterpene in the plant (Pareek et al. 2011). Parthenolide has been studied for its potential in treating inflammatory conditions, cardiovascular diseases, and cancer (Watson et al. 2009; Chadwick et al. 2013). Parthenolide has an α-methylene-γ-lactone ring and epoxide group, responsible for its biological effects including tumor treatment and lowering blood pressure in humans (Kupchan



**HATs** 

et al. 1971). The potential of parthenolide for the treatment of cancers has been confirmed which mainly resulted from its cytotoxicity to cancer cells as well as from targeting cancer stem cells (Ghantous et al. 2013). Aerial tissues of feverfew have parthenolide. The cytosolic compartment in glandular secretory trichome cells is responsible for synthesizing it (Majdi et al. 2011). Similar to other terpenes, the biosynthesis of parthenolide involves isopentenyl diphosphate (IDP) and dimethylallyl diphosphate (DMADP) precursors derived from the mevalonic acid (MVA) and methylerythritol phosphate (MEP) pathways (Majdi et al. 2011). The MVA pathway is located in the cytosol, while the MEP pathway is in the plastid (Dudareva et al. 2005). In the MVA pathway, two genes GAS and PTS are involved in parthenolide production. The first step in parthenolide biosynthesis, GAS catalyzes the farnesyl diphosphate to germacrene A. Subsequently, germacrene A is converted to germacrenoic acid by GAO, and then germacrenoic acid is converted to costunolide by COS. In the last step, PTS catalyzes costunolide to parthenolide (Majdi et al. 2011; Liu et al. 2014a). HDR, the initial pathway gene of terpene biosynthesis in the MEP pathway, is responsible for converting 1-hydroxy-2-methyl-2-(E)-butenyl 4-diphosphate (HMBDP) into IDP and DMADP (Huang et al. 2009). In plastidial terpenes, HDR can have a rate-limiting role in the biosynthesis of MEP-derived precursors (Hsieh and Goodman 2005). Due to the ability to transfer IDP from plastid to cytosol and vice versa, the MEP pathway might affect parthenolide production (Dudareva et al. 2005). Internal and external factors can affect the level of parthenolide in feverfew. One of the internal factors is chromatin structure, a complex of DNA and histone proteins, which plays an important role in gene expression and controlling transcriptional levels by adjusting the availability of DNA to the transcription factors (Klemm et al. 2019). In eukaryotes, chromatin comprises nucleosomes, with each nucleosome containing 147 bp of DNA around on an octameric core of two molecules each of histone H2A, H2B, H3, and H4 (Handy et al. 2011). The N-terminal tails of these histones undergo post-translational modifications, such as phosphorylation, ubiquitination, acetylation, and methylation (Yang et al. 2010). Histone acetylation influences chromatin structure and gene expression. Histone acetyltransferases (HATs) enzymes add acetyl groups to lysine residues on amine-terminals of histone. This process weakens interactions between histones, as well as between histones and DNA, thus increasing DNA accessibility to chromatin-binding proteins (Wang et al. 2014). On the other hand, histone deacetylases (HDACs) remove these modifications (Gräff and Tsai 2013). HATs activity led to relaxed chromatin and gene transcription, while deacetylation is associated with heterochromatin and gene repression (Shahbazian and Grunstein 2007). The interaction between

the HATs and HDACs controls developmental processes and stress responses (Wang et al. 2014; Liu et al. 2014a). In recent years, epigenetic modifications have become a central tool in the research and breeding of crops (Samantara et al. 2021). Studies about HDACs in plants have attracted more attention, especially the investigation of HDAC genes in Arabidopsis and other plant species (Ma et al. 2013). In plants, the HDAC family is divided into three families: RPD3/HDA1 (Reduced Potassium Dependency 3/histone deacetylase 1), SIR2 (Silent Information Regulator 2), and a plant-specific HD2 (histone deacetylase 2) (Wójcikowska et al. 2020; Kumar et al. 2021). HDAC enzymes require a zinc molecule as an essential cofactor in their binding site and are inhibited by Zn2+-binding HDAC inhibitors such as TSA (Kim and Bae 2011). TSA, a zinc-dependent histone deacetylase inhibitor, increases histone acetylation in chromatin, subsequently enhancing gene expression (Yoshida et al. 1995; Tan and Liu 2015). The hydroxamic group from TSA inhibits HDAC activity by binding to the zinc ion in class I and II HDACs. Since HDAC enzymes remove acetyl groups of lysine residues on amine-terminals of histone (Seto and Yoshida 2014), TSA with inhibition of HDACs can increase the hyperacetylation of histones, resulting in an open chromatin structure and the transcription of genes (Görisch et al. 2005). The application of TSA in plants causes increased histone acetylation and alters gene expression (Yang et al. 2010). In Arabidopsis, the treatment with TSA has increased in vitro somatic embryogenesis via the auxin-related pathway (Wójcikowska et al. 2018). In Brassica napus, the application of TSA and blocking HDAC activity leads to pollen cell embryogenesis (Li et al. 2014). TSA has increased cell division efficiency, callus proliferation, and adventitious shoot formation in the protoplast culture of Nicotiana benthamiana (Choi et al. 2023). Also, the effects of TSA on the division of mitosis in maize (Yang et al. 2010) and cold stress in Arabidopsis have been studied (Song et al. 2017). It was demonstrated that the use of TSA significantly enhances the efficiency of the wheat haploid doubling protocol (Jiang et al. 2017) and promotes the formation of embryonic callus and green shoots in this plant (Bie et al. 2020). In fungi, TSA treatment has increased the production of secondary metabolites (Shwab et al. 2007) and new meroterpenoids were identified from the cultures of Aspergillus terreus under the influence of TSA (Sun et al. 2018). The main objective of this study was to investigate the impact of seed treatment with different concentrations of TSA on increasing parthenolide production and the expression of genes related to its biosynthetic pathway in leaves of in vitro feverfew plantlets. Additionally, the impact of a foliar spray of in vivo feverfew plants with TSA on parthenolide production was investigated. The findings provide valuable insights into TSA's potential as an epigenetic



modulator for enhancing secondary metabolite production, advancing our understanding of strategies to manipulate plant biosynthetic pathways for improved yield and quality of medicinal compounds.

# **Materials and methods**

#### **Plant materials**

Feverfew seeds (*T. parthenium*. L) were provided from Zardband Company, Tehran, Iran.

# **Seed priming**

Before sowing, seeds were treated with different TSA concentrations including 0.1  $\mu$ M, 0.5  $\mu$ M, 1  $\mu$ M, and 2  $\mu$ M for 24 h at 4 °C. The treated seeds were then dried at room temperature. Additionally, some seeds were treated with distilled water in the same condition as a control.

#### In vitroseed culture.

Surface-sterilizing the pretreated seeds was done via immersion in 70% ethanol for 40 s and then submerging in 2% sodium hypochlorite for 5 min. Subsequently, the seeds were washed twice with sterile distilled water and aseptically cultured on a 1/4 strength MS medium (Murashige and Skoog, 1962) with 3% (w/v) sucrose, 0.8% (w/v) agar, and pH=5.7. The cultures were kept in a growth room at 25 °C under continuous light (approximately 40  $\mu$ mol m $^{-2}$ s $^{-1}$ , cool white fluorescent tubes). The in vitro seedlings obtained from the primed seeds are referred to as in vitro plants.

# Foliar spraying of in vivo plants with TSA

The non-treated seeds were sown in a seedling tray and then transferred to pots. The pots were kept in a greenhouse. The organization of pots was done in a completely randomized design (CRD) with three replications. For foliar spraying of TSA on in vivo feverfew plants, TSA solution at different concentrations (0.1  $\mu$ M, 0.5  $\mu$ M, 1  $\mu$ M, and 2  $\mu$ M) (pH 7.0) was sprayed on the leaves of 2-month-old plants until runoff. Some of the plants were sprayed with distilled water as a control (pH 7.0). Leaves were harvested at the following time points: 24, 48, and 72 h after spraying.

# **Quantification of parthenolide**

Feverfew leaves of 2-month-old plants for each replication were dried for 48 h at 65 °C and milled to a good powder using liquid nitrogen in a mortar and pestle. Afterward, ultrasonication-assisted extraction was done for 100 mg

of powdered leaves in 4 ml methanol for 18 min at room temperature for each replication. Each sample was centrifuged for 8 min at 4000 rpm and then the upper liquid was transferred to new vials. These vials were concentrated by a rotary evaporator (Heidolph, Germany) under vacuum at below 40 C. Dried methanol extracts were dissolved in a ratio of 10 mg/1 ml of pure methanol. So each replication was filtered through a 0.45 µm PTFE filters in new vials. From each replication, equal amounts (20 µl) were injected into the RP-HPLC-PDA system (Shimadzu, Japan), equipped with a reversed-phase 4.6 mm  $\times$  250 mm column. The mobile phase was an isocratic 10% methanol: 90% water at a 0.7 ml/min flow rate for 10 min. The UV detector was set at 210 nm. Calibration curve was obtained by running multiple injections of different concentrations of standard parthenolide (SIGMA).

# Gene expression analysis

For gene expression analysis, leaves of 2-month-old plants were ground in liquid nitrogen into powder with a mortar and pestle. Total RNA was extracted using the RNXPlus kit (SinaClon, Iran). Isolated RNA was treated with DNase I (SinaClon, IRAN). First-strand cDNA was synthesized with the 2-step Taqman Reverse (SinaClon First Strand cDNA synthesis) kit using 2 µg of total RNA based on the manufacturer's instructions. For gene expression analysis, real-time quantitative PCR (qRT-PCR), was done with a light cycler real-time 480 system (ROCHE, Switzerland) using the Sina Green HS-qPCR Mix, 2X (no ROX) (SinaClon, IRAN). The GAPDH was used as a housekeeping gene to normalize. The  $\Delta$ Ct method was used for RGE measurements. The  $\Delta$ Ct was calculated as follows:  $\Delta$ Ct = Ct (target gene) – Ct (GAPDH gene). The RGE obtained as: RGE=POWER (2; -ΔCt) (Livak and Schmittgen 2001). The qRT-PCR protocol was as follows: 15 min at 95 °C; followed by 40 cycles of denaturation for 20 s at 94 °C, annealing for 20 s at 59 °C, and elongation for 20 s at 72 °C, followed by melting curve analysis. The specific primer pairs (GAPDH, GAS, PTS, and HDR) were obtained from a published article (Majdi et al. 2015), and HDA19 (XM 010438600.2) Primer was designed with Primer3 (Table 1).

# Measurement of glandular trichomes density

The density of glandular trichomes on leaf surfaces was determined through a histochemical test involving concentrated H2SO4 (Liu and Liu 2012). Leaves from 2-month-old plants grown from TSA treated seeds were selected for this analysis. In each replication, the upper, middle, and lower leaves of the plant, were randomly selected. The leaves were placed on a glass slide and a drop of concentrated sulfuric



Table 1 Nucleotide sequences of primers used in real-time PCR

Transcript	Forward primer sequence	Reverse primer
		sequence
GAPDH	5`GTTGACTTGACTGT	5` CCTTGAGGTTG
	GAGACTTGAG	CCTTCGGATTC
GAS	5` TGCTATCTCGGGTA	5` TTCTCCTCTTAT
	CTTTCAAGG	TCTCAACTGTGC
PTS	5` GGCTGCATTTAACC	5` CTCGTTAGATGG
	TTCCCC	GCGTGTTG
HDR	5` CTGAGTGGCGTCAC	5`GAAGGGAGAAA
	AGATGG	CAGAGGAGATAGG
HDA19	5`CCAGCAAGATCAGA	5`TTGACAGAGCC
	TTCGCC	ACCAACAGA

acid was poured on the leaves. Samples were then placed under a microscope to observe the glandular trichomes. The density of glandular trichomes was measured in 1 mm<sup>2</sup> of adaxial areas in the leaves at 10x magnification using Digimizer (Version 5.4.9) image analyzing software.

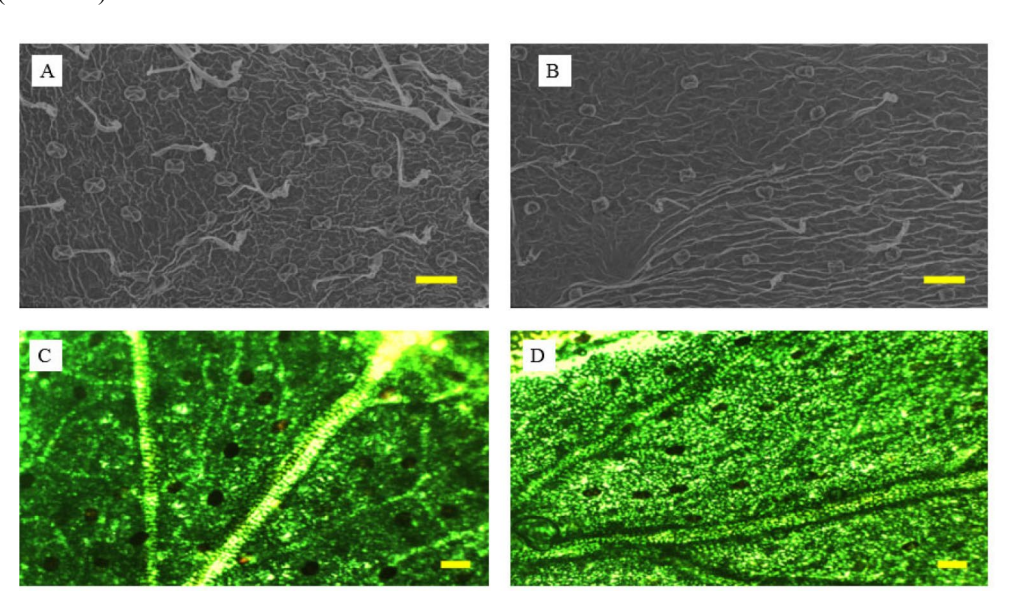
#### Microscopical investigation

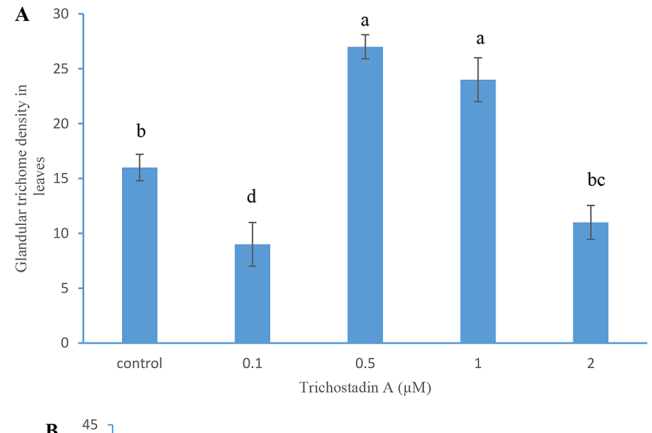
Scanning electron microscopy (SEM) was conducted following the method outlined by Krak and Mraz with slight modifications (Krak and Mráz, 2008). Leaves of 2-monthold plants grown from TSA treated seeds were dehydrated in an oven at 60 °C for 24 h and coated with a gold layer (500 Å). Samples were observed using a JEOL/JSM-840 A scanning electron microscope at 25 kV. For Optica imaging, freshly taken samples were examined with an Optika B9 Italy microscope.

#### **Data analysis**

A completely randomized design (CRD) with three replications was employed in experiments. Data were subjected to analysis of variance (ANOVA) to assess statistical

Fig. 1 Comparison of the density of glandular trichomes in leaves of in vitro plants treated with 0.5 μM TSA compared to control plants. a depicts the sample treated with 0.5 µM TSA, while **b** illustrates the control sample. The images were obtained using scanning electron microscopy, with a scale bar of 100 µm. Additionally, c presents the 0.5 µM TSA-treated sample, and d shows the control sample, as observed under scanning Optica microscopy, with a scale bar of 70 μm





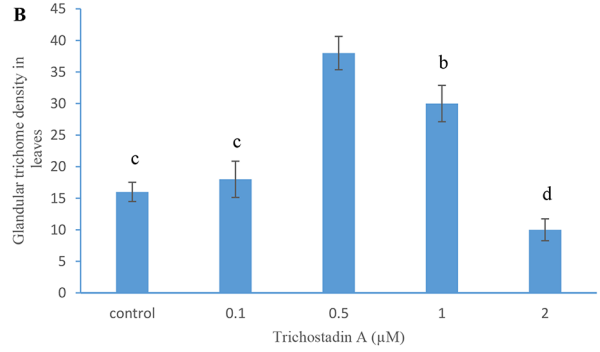


Fig. 2 Mean comparison of glandular trichome density in leaves of in vitro plants treated with various concentrations of TSA. Different letters indicate significant differences (P < 0.001) according to Duncan's test. Bars represent means  $(n=3) \pm S.E.$  the results of a display obtained from scanning Optical microscopy, while b presents results from scanning electron microscopy

significance. Multiple comparisons of means were conducted using Duncan's multiple tests with SPSS software.

#### Results

# Effect of seed pretreatment with TSA on the density of glandular trichomes in leaves of in vitro plants

In this research, the effect of different TSA concentrations on the density of glandular trichomes in leaves was investigated. The density of glandular trichomes in leaves of in vitro 2-month-old plants was assessed using scanning electron microscopy (SEM) and the Optika B9 Italy microscope (Fig. 1). Analysis of the data using light microscopy showed significant differences among various TSA treatments for glandular trichome density (P < 0.001). Compared to control plants, significant differences in glandular trichome density were observed at 0.5µM and 1µM TSA, while 2µM TSA showed density similar to the control, and the lowest density of glandular trichomes was observed at 0.1 µM TSA (Fig. 2a). Notably, the density of glandular trichomes in leaves of plants treated with 0.5µM and 1µM TSA increased to 1.6 and 1.5 times higher, respectively, than that of control plants.

The results of the ANOVA for electron microscopy were consistent with those obtained from light microscopy. The highest density of glandular trichomes was observed at 0.5µM compared to its respective control and other TSA treatments. Moreover, the results indicated that the density of glandular trichomes at 0.1 µM TSA was similar to that of the control. Furthermore, there was an increase in the density of glandular trichomes at 1µM TSA compared to its control counterpart; however, at 2µM, there was a significant decrease in trichome density. Specifically, these values were 1.1 (0.1 $\mu$ M), 2.3 (0.5 $\mu$ M), 1.8 (1 $\mu$ M), and 0.6 (2μM) times higher than those observed in untreated plants (Fig. 2b).

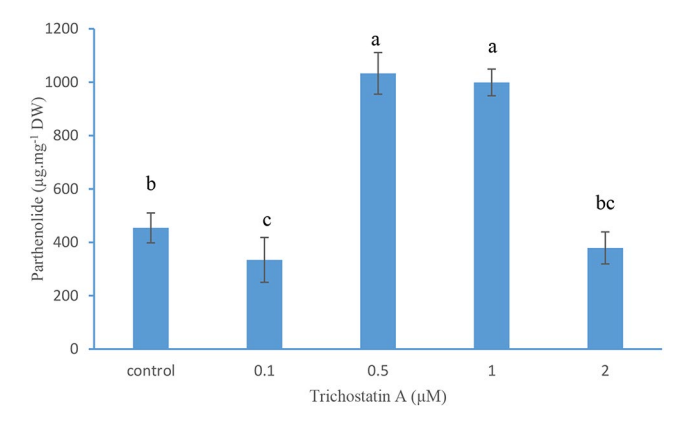


Fig. 3 Parthenolide content (μg·mg<sup>-1</sup> DW) in the leaves of T. parthenium in vitro plants treated with TSA. Different letters indicate significant differences (p < 0.001) according to Duncan's test. Bars represent means  $(n=3) \pm S.E$ 

# Effect of seed pretreatment with TSA on parthenolide production in leaves of in vitro plants

The effects of different TSA concentrations on the content of parthenolide, a major secondary metabolite of feverfew, were investigated in this experiment. The results of the ANOVA indicated a significant impact of TSA concentrations on parthenolide content. In the leaves of in vitro plants, the parthenolide content at concentrations of 0.1, 0.5, 1, and 2 µM TSA was measured as 334.2, 1033.5, 999.3, and 379.6 µg/mg DW, respectively. The highest parthenolide concentration was observed at 0.5µM and 1µM (P < 0.001) (Fig. 3). Parthenolide accumulation in leaves of TSA-treated plants with 0.5µM and 1µM increased to 2.27 and 2.2 times higher than that of control plants, respectively. There was no significant difference in parthenolide accumulation between the  $0.1\mu M$  and  $2\mu M$  TSA treatments and the control (Fig. 3).

# Effect of seed pretreatment with TSA on the expression of parthenolide biosynthesis pathway genes in leaves of in vitro plants

Gene expression analysis using qPCR was carried out to understand how TSA affects parthenolide biosynthesis and the relationship between gene expression and parthenolide accumulation. The study found that the expression of genes involved in the parthenolide biosynthetic pathway, including GAS and PTS of the MVA pathway, the HDR gene in the MEP pathway, and a histone deacetylase gene (HDA19), exhibited significant changes in response to TSA. The expression levels of GAS significantly increased at concentrations of 0.5µM and 1µM TSA, reaching 1.48 and 1.4 times that of control plants, respectively. Conversely, the expression of GAS at 0.1µM and 2µM TSA was significantly decreased and resembled that of control plants (Fig. 4a). Similarly, the expression pattern of PTS increased significantly with all concentrations of TSA compared to the control. The treatment with 0.5 µM TSA produced the highest transcript levels of the PTS gene, which were 1.69 times higher than those in untreated plants. Although the expression of the PTS gene decreased significantly at concentrations of 0.1 µM, 1µM, and 2µM TSA, it remained significantly higher than in control plants (Fig. 4b). Regarding the HDR gene, its expression levels decreased significantly at a concentration of 0.1µM TSA compared to the control (Fig. 4c). However, there was no significant difference in gene expression levels between the 0.5µM and 1µM TSA treatments and the control. Interestingly, the expression pattern of HDR increased significantly at 2µM TSA, reaching 2.12 times higher levels than in untreated plants (Fig. 4c). Furthermore, the expression pattern of the HDA19 gene



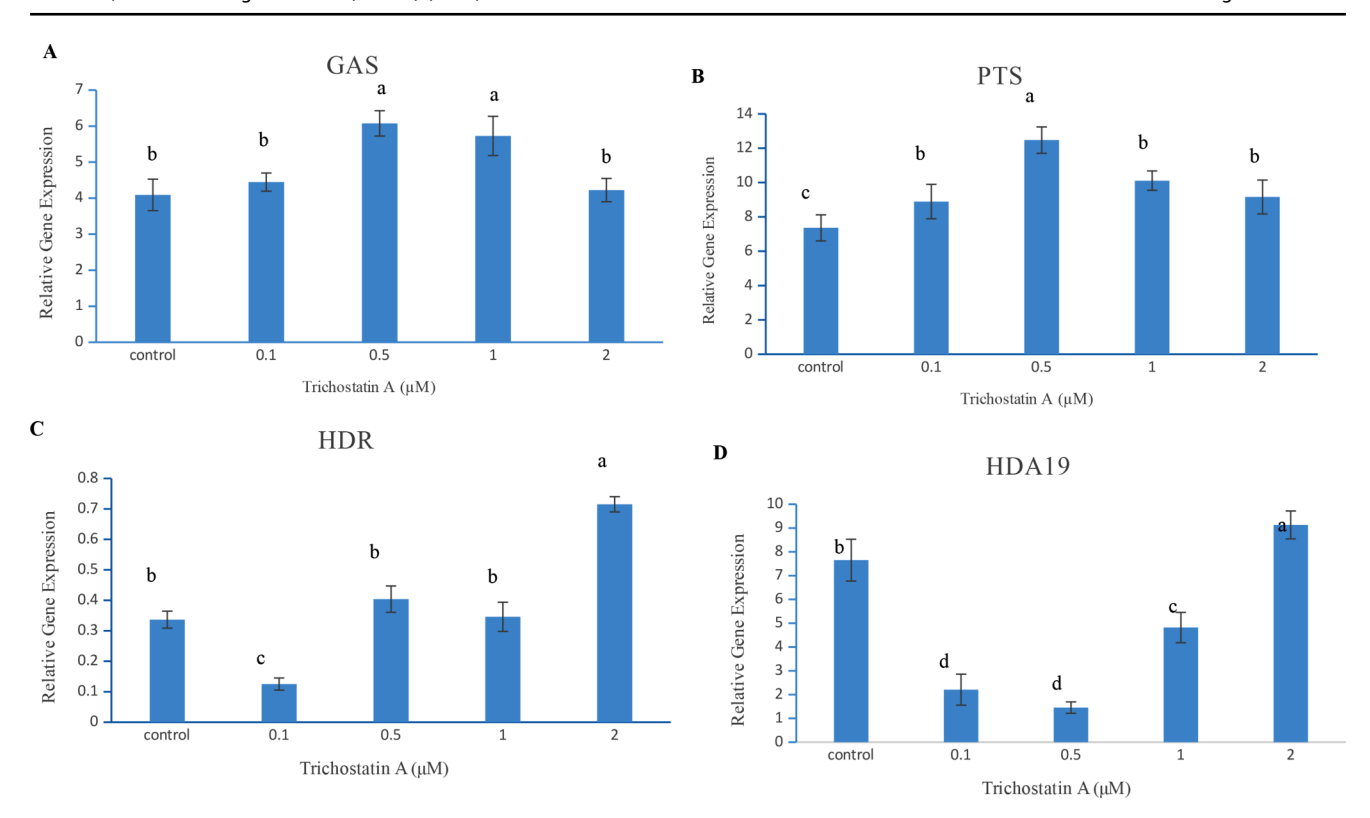


Fig. 4 Relative gene expression (RGE) of two parthenolide biosynthetic pathway genes, namely a: GAS and b: PTS, as well as c: an initial terpene biosynthesis pathway gene (HDR), and d: HDA19 gene, acting as a histone deacetylase, were assessed in both control (untreated) and TSA-treated in vitro plants. Real-time quantitative PCR (qPCR)

decreased significantly at concentrations of  $0.1\mu M$ ,  $0.5\mu M$ , and  $1\mu M$  TSA compared to the control (Fig. 4d). The highest transcript levels of the HDA19 gene were observed at  $2\mu M$  TSA (P<0.001), showing a 1.19-fold increase compared to control plants (Fig. 4d).

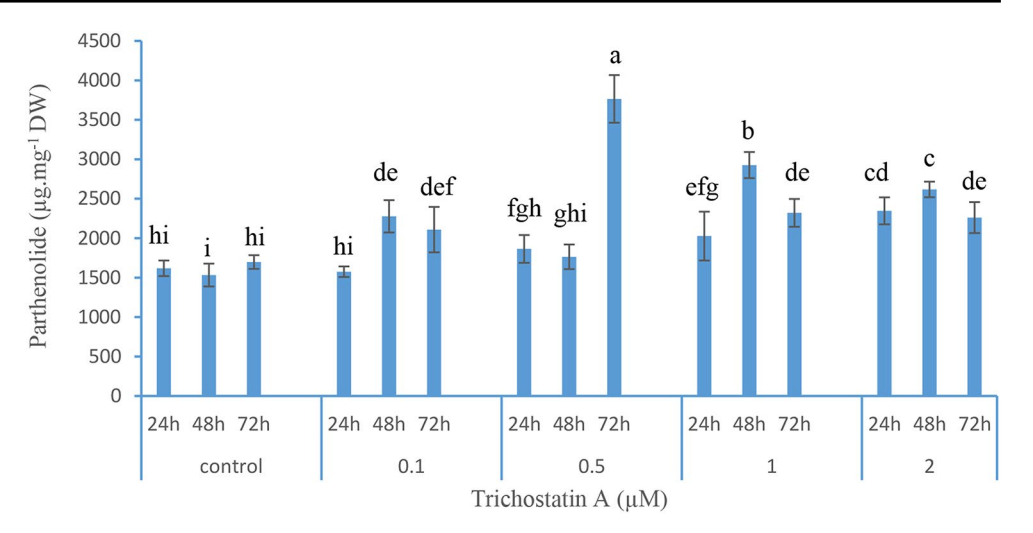
# Effect of foliar spraying of in vivo plants with TSA on parthenolide accumulation

The effect of foliar spraying with different concentrations of TSA on parthenolide production in in vivo plants was investigated in this experiment. The results of the ANOVA indicated that the concentrations of TSA, the parthenolide extraction times after TSA treatments, and their interaction all had significant effects on parthenolide levels in the leaves of treated feverfew plants (P < 0.001). Throughout the time-course experiment, parthenolide accumulation exhibited a steady concentration in control plants. No significant difference in parthenolide content was observed in control plants during the time series of the experiment (P > 0.05) (Fig. 5). Following 24 h of foliar spraying with  $0.1 \mu M$  TSA, there were no significant differences in parthenolide content compared to the control plants. However, after 48 h, the parthenolide amount ( $2277 \mu g \cdot mg^{-1}$  DW) increased

analysis was conducted based on the Ct values. GAPDH, serving as a housekeeping gene, was utilized to normalize the Ct values for each sample. Bars labeled with different letters indicate significant differences (p < 0.001), as determined by Duncan's test. Error bars represent means (n = 3)  $\pm$  S.E

significantly, reaching a level 1.48 times higher than in control plants. Subsequently, at 72 h after TSA foliar spraying, parthenolide accumulation decreased but remained significantly higher than in control plants (1.18 times) (Fig. 5). After foliar spraying with 0.5µM TSA, no significant difference in parthenolide content was observed compared to control plants at 24 and 48 h. However, the highest amount of parthenolide (3765.45 µg·mg<sup>-1</sup> DW) was detected 72 h after treatment with 0.5 µM TSA, which was 2.21 times higher than in untreated plants (Fig. 5). When 1µM TSA was used, the parthenolide contents increased at 24 and 48 h after spraying, but decreased at 72 h, although it remained significantly higher than in the control plants. The parthenolide amounts at 24, 48, and 72 h were 2027.5, 2927.34, and 2320.23 μg·mg<sup>-1</sup> DW, respectively, which were 1.25, 1.91, and 1.36 times higher than in control plants (Fig. 5). The impact of foliar spraying with 2µM TSA on parthenolide production increased at 24, 48, and 72 h. The amounts of parthenolide were 2347.54, 2618.12, and 2261.33 μg·mg-1 DW, respectively, which were 1.45, 1.7, and 1.33 times higher than in control plants (Fig. 5).





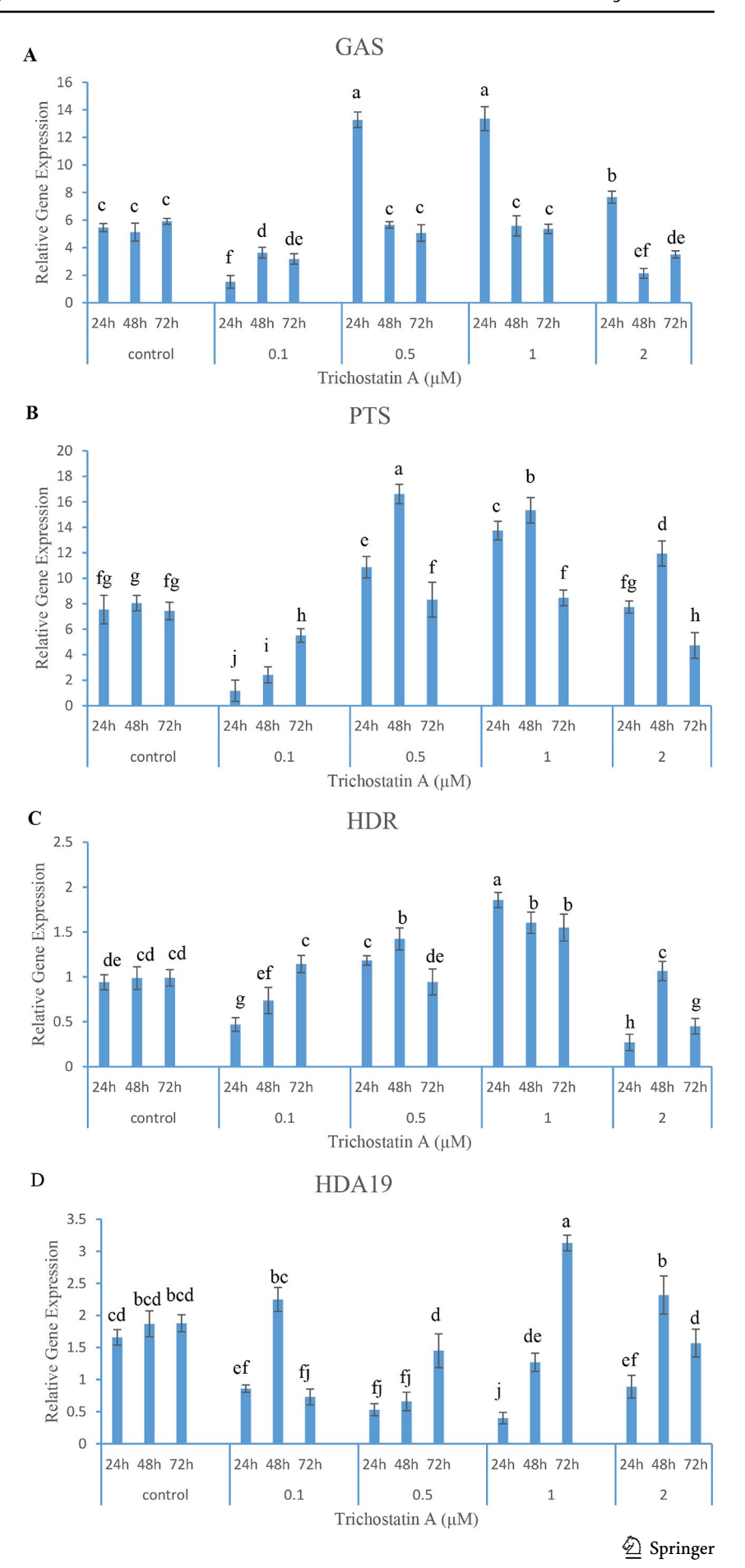
# Effect of foliar spraying of in vivo plants with TSA on the expression levels of parthenolide biosynthesis pathway genes

To assess the effect of TSA on parthenolide biosynthesis and the relationship between gene expression and parthenolide accumulation, real-time PCR was employed to identify changes in the transcript levels of GAS and PTS from the MVA pathway, HDR gene from the MEP pathway, and HDAC19, which is a histone deacetylase gene. Transcript levels were evaluated in leaves of feverfew plants that were sprayed with various concentrations of TSA, water was used as control, at three time-points of 24 h, 48 h, and 72 h after spraying. ANOVA analysis revealed significant (P < 0.001) differences among TSA concentrations, various time points, and their interaction for the transcription levels of all genes in the leaves of feverfew plants. Throughout the different time series, no significant difference was observed for transcription levels of all studied genes in control plants (P>0.05). Using 0.1µM TSA, the transcription level of the GAS gene significantly decreased. At this concentration of TSA, the expression levels of GAS at 24 h, 48 h, and 72 h time points were lower than those of the control (Fig. 6a). Foliar spraying with 0.5µM and 1µM TSA increased the expression level of the GAS gene. The highest expression levels of the GAS gene were detected 24 h after treatment with 0.5µM and 1µM TSA, which were 2.43 and 2.45 times higher than those in untreated plants (Fig. 6a). However, the expression level of the GAS gene decreased at 48 h and 72 h time points and, returning to the level of control plants (Fig. 6a). When plants were foliar sprayed with 2μM TSA, the expression level of GAS was significantly increased 24 h after treatment, which was 1.4 times higher than in control plants (Fig. 6a). The expression level of the GAS gene decreased at 48 h and 72 h, reaching a lower level than that of the control plants (Fig. 6a). Regarding the PTS gene,

foliar spraying of the plants with 0.1 µM TSA decreased the expression level of this gene after 24 h. However, after 48 h and 72 h from the initial treatment, the expression levels increased, but remained lower than those of the control plants (Fig. 6b). After treating the plants with 0.5µM and 1μM TSA, the expression levels of the PTS gene significantly increased at 24 h and 48 h time points. The highest level of PTS transcript was observed 48 h after treatment with 0.5µM TSA, which was 2.06 times higher than that in control plants. For 1µM TSA PTS transcript level was 1.9- fold higher than control plants. However, after 72 h, the level of PTS transcription dropped and declined to the level of control plants for both TSA concentrations (Fig. 6b). The level of PTS transcription was not significantly different from control plants 24 h after foliar spraying with 2µM TSA. However, after 48 h, the expression level of the gene increased significantly (1.48-fold higher than in control plants). After 72 h, the expression level of PTS decreased compared to control plants (Fig. 6b). The effect of foliar spraying of feverfew plants with different TSA concentrations on HDR gene expression levels showed that 0.1µM TSA at 24 and 48 h significantly decreased the expression levels of this gene compared to control plants. The expression level of HDR at these time points was lower than that of the control. However, the expression level of this gene increased at 72 h and reached the level of control plants (Fig. 6c). Twenty-four hours after spraying the plants with 0.5μM TSA, there was no change in the transcription level of the HDR gene compared to the control plants. However, after 48 h, the expression level of the gene increased significantly, which was 1.44 times higher than control plants. Subsequently, at 72 h after foliar spraying, the expression level decreased and reached a lower level than the control plants (Fig. 6c). When 1µM TSA was used, the expression level of HDR at 24 h increased to 1.96 times higher than the control plants. The highest HDR transcript level was observed 24 h after treatment with 1µM TSA. At 48 h and



Fig. 6 The effects of foliar spraying of different TSA concentrations on in vivo plants and different time points of sampling, on relative gene expression (RGE) of two parthenolide biosynthetic pathway genes, including a: GAS and b: PTS, as well as c: an initial terpene biosynthesis pathway gene (HDR), and d: HDA19 as a histone deacetylase gene on the levels of in vivo plants. Real-time quantitative PCR (qPCR) was conducted based on the Ct values, with GAPDH serving as a housekeeping gene to normalize the Ct value for each sample. Bars labeled with different letters indicate significant differences (p < 0.001) according to Duncan's test. Error bars represent means (n = 3)  $\pm$  S.E



72 h time points, the expression levels of HDR decreased but they were still significantly higher than those of control plants (1.6 and 1.5 times that of control plants, respectively) (Fig. 6c). The application of 2µM TSA decreased the expression level of HDR at 24 h, which was lower than that of the control plants. However, after 48 h, the expression level of the gene increased to the level of control plants, and at 72 h, the level of gene expression decreased again, which was lower than that of the control plants (Fig. 6c). The analysis of the expression of the HDA19 gene after spraying with different concentrations of TSA showed that 24 h after using 0.1µM TSA, the gene's transcript level decreased significantly compared to the control plants. After 48 h, the expression levels increased and reached that of the control plants. However, at 72 h, the gene expression level decreased again compared to the control plants (Fig. 6d). By treating with 0.5µM TSA, the expression level of HDA19 decreased at 24 and 48 h, lower than in the control plants. However, after 72 h, the gene expression level increased and matched the control plants (Fig. 6d). When treated with 1µM TSA, the expression of HDA19 decreased at 24 h and then returned to the control level at 48 h. At 72 h post-treatment with 1 µM TSA, the expression level of the HDA19 gene increased to 1.66 times higher than in the control plants, reaching the highest HDA19 transcript level (Fig. 6d). Foliar spraying of feverfew plants with 2µM TSA decreased the expression level of the HDA19 gene after 24 h. However, the expression levels subsequently increased and returned to the control plant levels at 48 and 72 h (Fig. 6d).

# **Discussion**

Our study demonstrates that treating seeds with TSA has a significant impact on the biosynthesis and accumulation of parthenolide in the leaves of T. parthenium under in vitro conditions. Our findings indicate that levels of 0.5µM and 1μM TSA increased the density of glandular trichomes (Fig. 2). Glandular trichomes, specialized epidermal appendages in plants, are well-known for synthesizing and releasing secondary metabolites such as terpenoids, flavonoids, methyl ketones, and acyl sugars (Ashrafi et al. 2022). Various phytohormones, including auxins, cytokinins, gibberellins, jasmonates, and brassinosteroids, can influence epidermal differentiation programs, leading to increased trichome density in plants like Artemisia annua (Maes et al. 2011). Additionally, specific growth regulators in the culture medium can enhance glandular trichome density in Stevia rebaudiana (Ashrafi et al. 2022).

In another study, it was found that the symbiosis *Arbus-cular mycorrhizal* fungi with *Stevia rebaudiana* led to an increase in trichome density and the accumulation of

secondary metabolite (Sarmiento-López et al. 2021). The primary stages of trichome development are regulated by the TRANSPARENT TESTA GLABRA 1 (TTG1) gene (Larkin et al. 1994; Ioannidi et al. 2016). A previous study on Arabidopsis thaliana indicated that biotic and abiotic factors can influence the regulation of the TTG1 gene and ultimately affect trichome density on leaves (Larkin et al. 1994). Sarmiento-López et al. (2021) reported a correlation between increased expression levels of TTG1 and an increase in trichome density on leaves from S. rebaudiana-colonized plants. Our results indicated that TSA can increase gene expression profiles, potentially influencing genes associated with trichome development, particularly the TTG1 gene, leading to an increase in trichome numbers on the leaves of *T. parthenium*. In our study, HPLC analysis indicated that 0.5µM and 1µM TSA had the most significant impact on parthenolide accumulation (Fig. 3). Considering that glandular trichomes are known as biochemical factories for the production and accumulation of secondary metabolites (Huchelmann et al. 2017), our observations suggest that TSA may directly or indirectly increase trichome density and parthenolide accumulation in *T. parthenium*. Our results also indicate that TSA influences the expression of GAS and PTS from the MVA pathway, the HDR gene from the MEP pathway, and HDA19 as a histone deacetylase. The inhibition of HDACs by TSA has increased acetylation on lysine, neutralizing the positive charge of histones and reducing the interaction between histones and DNA (Bannister and Kouzarides 2011). It leads to the loosening of chromatin, making the DNA sequence accessible to transcription factors and RNA polymerase, and increases the expression of genes (Bannister and Kouzarides 2011). The expression of the studied genes from the MVA pathway, which was stimulated by TSA, may be associated with parthenolide accumulation. Our study showed that the GAS gene was upregulated by 0.5µM and 1µM TSA, and the expression of PTS increased with 1µM TSA. The expression levels of GAS and PTS are closely related to parthenolide biosynthesis. Although HDR was affected differently by TSA treatments, its expression did not show the same pattern as parthenolide accumulation. The expression of HDA19 increased with 2µM TSA (Fig. 4). Darbahani et al. (2022) reported that nanoparticles (Aluminum Oxide alpha (Al2O3) and Magnesium Aluminate Spinel (Mg Al2O4) caused an increase in the expression of the GAS gene and other genes in the parthenolide biosynthesis pathway, and the expression of GAS correlated with parthenolide accumulation in Feverfew. In a study by Majdi et al. (2015), it was demonstrated that Feverfew with high expression of TpGAS in glandular trichomes showed a significant correlation with high concentrations of parthenolide. In the protoplast culture of Nicotiana benthamiana, TSA has increased cell division efficiency, callus proliferation, and



adventitious shoot formation (Choi et al. 2023). It was also shown that TSA increased the expression of Cyclin-dependent kinase (CDK), Cyclin D3-1 (CYCD3-1), cell cycle regulatory genes, and WUSCHEL (WUS) genes in the protoplast culture of *Nicotiana benthamiana* (Choi et al. 2023). In a previous study, TSA-induced somatic embryogenesis in Arabidopsis indicated that TSA affected the expression level of several genes encoding transcription factors including LEC1, LEC2, BBM, and stress responses (MYB118) and increased the expression of these genes in the TSA-treated explants (Wójcikowska et al. 2018). In the second experiment, plants were sprayed with different concentrations of TSA. Investigations at three time points (24 h, 48 h, and 72 h after treatment) showed an increase in the expression of GAS at 24 h after treatment with 0.5 uM and 1 uM TSA (Fig. 6a), an increase in the expression of PTS at 48 h after treatment with 0.5µM TSA (Fig. 6b), an increase in HDR expression at 24 h after treatment with 1µM TSA (Fig. 6c), and induced the highest expression of HDA19 at 72 h after treatment with 1µM TSA (Fig. 6d). Additionally, the highest accumulation of parthenolide was observed at 72 h after treatment with 0.5 µM TSA (Fig. 5). In this experiment, a positive correlation was observed between the expression of GAS and PTS genes and the accumulation of parthenolide. These results are consistent with the findings of previous researchers (Darbahani et al. 2022).

HDA19, belonging to RPD3/HDA1, is involved in germination, flowering, biotic and abiotic stress responses, and zygotic embryos (Wójcikowska et al. 2020; Kumar et al. 2021). HDAC enzymes require a zinc molecule as an essential cofactor in their binding site and are inhibited by Zn2+binding HDAC inhibitors such as TSA (Kim and Bae 2011). Inhibition of HDACs by TSA leads to an increase in acetyl groups on histones, resulting in hyperacetylation and a more open chromatin structure associated with enhanced gene expression (Görisch et al. 2005). The results of this research showed that TSA increased HDAC19 gene expression in all concentrations, especially after 48–72 h of initial treatment. These results are attributed to the positive effect of TSA on the opening of chromatin structure. Additionally, the results of this research, as well as previous researches, show that TSA has an inhibitory effect on histone deacetylase enzyme and not on the gene responsible for it, as its inhibitory mechanism was mentioned above. In the protoplast culture of Nicotiana benthamiana, TSA has enhanced histone H3 acetylation levels (Choi et al. 2023). Furthermore, treating Arabidopsis seedlings with TSA has been shown to increase H3K9/K14Ac and H4K5Ac epigenetic marks (Venturelli et al. 2015; Mengel et al. 2017). The reduction of HDAC activity up to two times lower than the freshly isolated tissues of Arabidopsis explants cultured on somatic embryogenesis induction media has been indicated with the application of 1µM TSA (Wójcikowska et al. 2018). Treatment with 1µM TSA increased the expression level of the AhHDA1 gene of Arachis hypogaea L. compared to control (Su et al. 2015). Moreover, the expression levels of transcription factor genes (AhAREB1, AhDREB2A-like, AhWRKY33-like) increased with 1µM TSA in Arachis hypogaea L. (Su et al. 2015). It has been demonstrated that TSA can upregulate gene transcription profiles during in vitro somatic embryogenesis in Arabidopsis (Wójcikowska et al. 2018) and Brassica napus (Li et al. 2014). In Picea abies, the use of TSA during the maturation of embryogenic cultures has halted the maturation process, and maintained the expression levels of PaHAP3A and PaVP1 (Uddenberg et al. 2011). Furthermore, Nowak et al. (2024) reported that TSA treatment in barley in vitro cultures resulted in enhanced expression levels of LEC1, FUS3, BBM, PHB, and ERF022 genes (Transcription factor) in barley in vitro cultures. Additionally, the expression levels of HDA19 and HDA6 have been shown to increase in response to TSA. Similarly, TSA has increased the expression of HDA19 in Arabidopsis (Morończyk et al. 2022) and the expression of HDACs in grapevine (Martínez et al. 2021) and wheat (Valero-Rubira et al. 2023). In several previous studies on the production of secondary metabolites by fungi, it has been demonstrated that TSA enhances the chemical diversity of secondary metabolites (Williams et al. 2008). Fungi treated with 1 μM trichostatin A showed increased production of secondary metabolites in cultures of Penicillium expansum and Alternaria alternata (Shwab et al. 2007). Additionally, in Aspergillus clavatus, TSA at 0.5 µM increased secondary metabolites (Zutz et al. 2013). Furthermore, four new meroterpenoids were isolated after the treatment of the culture medium of Aspergillus terreus with 10µM TSA (Sun et al. 2018). Kooke et al. (2019) analyzing QTL data in Arabidopsis reported that epigenetics might play an important role in regulating the accumulation of secondary metabolites. Our findings show that TSA, as an epigenetic modulator, can have a positive impact on the expression of GAS and PTS genes in the parthenolide biosynthesis pathway. The increased expression of GAS and PTS is likely linked to higher parthenolide accumulation. Our results indicate that concentrations of 0.5 µM and 1 μM of TSA can lead to an increase in parthenolide levels. A lower concentration of TSA (0.1 µM) had a smaller effect on parthenolide production, while a higher concentration (2 μM) caused a reduction in parthenolide production in Feverfew plants, possibly due to its toxicity.



# **Conclusion**

In conclusion, our investigation into the impact of exogenous Trichostatin A (TSA) application on the expression of genes associated with parthenolide biosynthesis and accumulation in feverfew (T. parthenium) provides valuable insights into the regulation of secondary metabolite production in plants. This study revealed that TSA, an inhibitor of histone deacetylases (HDACs), positively influenced the expression of key genes, including Germacrene A synthase (GAS) and parthenolide synthase (PTS), as well as the density of glandular trichomes, leading to an enhanced production of parthenolide. The results were consistent across two experimental approaches: seed priming under in vitro conditions and foliar spray on in vivo Feverfew plants. The findings suggest a potential role for TSA as a tool to modulate plant secondary metabolism and improve the yield of valuable metabolites, such as parthenolide. The positive correlation between TSA concentration and parthenolide accumulation, along with the differential expression of biosynthetic genes, highlights the intricate regulatory mechanisms involved in the biosynthesis of secondary metabolites. Furthermore, the study underscores the importance of epigenetic modifications, specifically histone acetylation, in influencing gene expression and, consequently, the production of bioactive compounds in medicinal plants. This research contributes to the growing knowledge of the application of epigenetic modulators in plant biotechnology, providing a foundation for further exploration of strategies to enhance the production of bioactive compounds with pharmaceutical and therapeutic potential. The detailed understanding of the molecular mechanisms uncovered in this study opens avenues for targeted approaches to manipulate secondary metabolite pathways in plants for improved yield and quality of medicinal compounds.

Author contributions MRA, AM, and MA conceived and designed the experiments. MA carried out all experiments and wrote the original. draft. MA and DD carried out the metabolomic analyses. MA and MRA analyzed the data. MRA and AM edited the manuscript. All authors approved the final version.

Data availability The data will be made available on reasonable request.

#### **Declarations**

**Conflict of interest** The authors confirm that there are no known conflicts of interest associated with this publication.

# References

Ashrafi K, Iqrar S, Saifi M, Khan S, Qamar F, Quadri SN, Abdin MZ (2022) Influence of plant growth regulators on glandular trichome density and steviol glycosides Accumulation in

- Stevia rebaudiana. ACS Omega 7(35):30967–30977. https://doi.org/10.1021/acsomega.2c02957
- Bannister AJ, Kouzarides T (2011) Regulation of chromatin by histone modifications. Cell Res 21(3):381–395. https://doi.org/10.1038/cr.2011.22
- Bie XM, Dong L, Li XH, Wang H, Gao XQ, Li XG (2020) Trichostatin A and sodium butyrate promotes plant regeneration in common wheat. Plant Signal Behavi 15(12):1820681. https://doi.org/10.1080/15592324.2020.1820681
- Chadwick M, Trewin H, Gawthrop F, Wagstaff C (2013) Sesquiterpenoids lactones: benefits to plants and people. Int J Mol Sci 14(6):12780–12805. https://doi.org/10.3390/ijms140612780
- Choi SH, Ahn WS, Lee MH, Jin DM, Lee A, Jie EY, Ju SJ, Ahn SJ, Kim SW (2023) Effects of TSA, NaB, Aza in Lactuca sativa L. protoplasts and effect of TSA in Nicotiana Benthamiana protoplasts on cell division and callus formation. PLoS ONE 24(2):e0279627. https://doi.org/10.1371/journal.pone.0279627
- Darbahani M, Rahaie M, Ebrahimi A, Khosrowshahli M (2022) The effects of several abiotic elicitors on the expression of genes of key enzymes involved in the parthenolide biosynthetic pathway and its content in feverfew plant (Tanacetum parthenium L). Nat Prod Res 36(23):6132–6136. https://doi.org/10.1080/14786419.2 022.2055555
- Dudareva N, Andersson S, Orlova I, Gatto N, Reichelt M, Rhodes D, Gershenzon J (2005) The nonmevalonate pathway supports both monoterpene and sesquiterpene formation in snapdragon flowers. Proc Natl Acad Sci 102(3):933–938. https://doi.org/10.1073/pnas.0407360102
- Ghantous A, Sinjab A, Herceg Z, Darwiche N (2013) Parthenolide: from plant shoots to cancer roots. Drug Discovery Today 18(17–18):894–905. https://doi.org/10.1016/j.drudis.2013.05.005
- Görisch SM, Wachsmuth M, Tóth KF, Lichter P, Rippe K (2005) Histone acetylation increases chromatin accessibility. J Cell Sci 118(24):5825–5834. https://doi.org/10.1242/jcs.02689
- Gräff J, Tsai LH (2013) Histone acetylation: molecular mnemonics on the chromatin. Nat Rev Neurosci 14:97–111. https://doi.org/10.1038/nrn3427
- Handy DE, Castro R, Loscalzo J (2011) Epigenetic modifications: basic mechanisms and role in cardiovascular disease.

  Circulation 123(19):2145–2156. https://doi.org/10.1161/

  CIRCULATIONAHA.110.956839
- Hsieh MH, Goodman HM (2005) The Arabidopsis IspH homolog is involved in the plastid nonmevalonate pathway of isoprenoid biosynthesis. Plant Physiol 138:641–653. https://doi.org/10.1104/pp.104.058735
- Huang JZ, Cheng TC, Wen PJ, Hsieh MH, Chen FC (2009) Molecular characterization of the Oncidium orchid HDR gene encoding1hydroxy-2-methyl-2-(E)-butenyl 4-diphosphate reductase, the last step of the methylerythritol phosphate pathway. Plant Cell Rep 28:1475–1486. https://doi.org/10.1007/s00299-009-0747-6
- Huchelmann A, Boutry M, Hachez C (2017) Plant glandular trichomes: natural cell factories of high biotechnological interest. Plant Physiol 175(1):6–22. https://doi.org/10.1104/pp.17.00727
- Ioannidi E, Rigas S, Tsitsekian D, Daras G, Alatzas A, Makris A, Kanellis AK (2016) Trichome patterning control involves TTG1 interaction with SPL transcription factors. Plant Mol Biol 92:675–687. https://doi.org/10.1007/s11103-016-0538-8
- Jiang F, Ryabova D, Diedhiou J, Huel P, Randhawa H, Marillia EF, Kathiria P (2017) Trichostatin A increases embryo and green plant regeneration in wheat. Plant Cell Rep 36:1701–1706. https://doi. org/10.1007/s00299-017-2183-3
- Kim HJ, Bae SC (2011) Histone deacetylase inhibitors: molecular mechanisms of action and clinical trials as anti-cancer drugs. Am J Transl Res 3(2):166–179



- Klemm SL, Shipony Z, Greenleaf WJ (2019) Chromatin accessibility and the regulatory epigenome. Nat Revi Gene 20(4):207-220. https://doi.org/10.1038/s41576-018-0089-8
- Kooke R, Morgado L, Becker F, van Eekelen H, Hazarika R, Zheng Q, de Vos RC, Johannes F, Keurentjes JJ (2019) Epigenetic mapping of the Arabidopsis metabolome reveals mediators of the epigenotype-phenotype map. Genome Res 29(1):96-106. http:// www.genome.org/cgi/doi/https://doi.org/10.1101/gr.232371.117
- Kumar V, Thakur JK, Prasad M (2021) Histone acetylation dynamics regulating plant development and stress responses. Cell Mol Life Sci 78:4467–4486. https://doi.org/10.1007/s00018-021-03794-x
- Kupchan SM, Eakin MA, Thomas AM (1971) Tumor inhibitors. 69. Structure-cytotoxicity relations among the sesquiterpene lactones. J Medic Chemis 14(12):1147–1152. https://doi.org/10.1021/ jm00294a001
- Larkin JC, Oppenheimer DG, Lloyd AM, Paparozzi ET, Marks MD (1994) Roles of the GLABROUS1 and TRANSPARENT TESTA GLABRA genes in Arabidopsis trichome development. Plant Cell 6(8):1065-1076. https://doi.org/10.1105/tpc.6.8.1065
- Li H, Soriano M, Cordewener J, Muiño JM, Riksen T, Fukuoka H, Boutilier K (2014) The histone deacetylase inhibitor trichostatin a promotes totipotency in the male gametophyte. Plant Cell 26(1):195-209. https://doi.org/10.1105/tpc.113.116491
- Liu M, Liu J (2012) Structure and histochemistry of the glandular trichomes on the leaves of Isodon rubescens (Lamiaceae). Afr J Biotechnol 11(17):4069-4078. https://doi.org/10.5897/AJB11.4024
- Liu X, Yang S, Zhao M, Luo M, Yu CW, Chen CY, Wu K (2014) Transcriptional repression by histone deacetylases in plants. Mole Plant 7(5):764-772. https://doi.org/10.1093/mp/ssu033
- Liu O. Manzano D. Tanic' N. Pesic M. Bankovic J. Pateraki I. Ricard L, Ferrer A, de Vos R, van de Krol S, Bouwmeester H (2014a) Elucidation and in planta reconstitution of the parthenolide biosynthetic pathway. Metab Eng 23:145–153. https://doi.org/10.1016/j. ymben.2014.03.005
- Ma X, Lv S, Zhang C, Yang C (2013) Histone deacetylases and their functions in plants. Plant Cell Rep 32:465-478. https://doi. org/10.1007/s00299-013-1393-6
- Maes L, Van Nieuwerburgh FC, Zhang Y, Reed DW, Pollier J, Vande Casteele SR, Goossens A (2011) Dissection of the phytohormonal regulation of trichome formation and biosynthesis of the antimalarial compound artemisinin in Artemisia annua plants. New Phytol 189(1):176-189. https://doi. org/10.1111/j.1469-8137.2010.03466.x
- Majdi M, Liu Q, Karimzadeh G, Malboobi MA, Beekwilder J, Cankar K, Bouwmeester H (2011) Biosynthesis and localization of parthenolide in glandular trichomes of feverfew (Tanacetum parthenium L. Schulz Bip). Phytochemistry 72(14–15):1739–1750. https://doi.org/10.1016/j.phytochem.2011.04.021
- Majdi M, Abdollahi MR, Maroufi A (2015) Parthenolide accumulation and expression of genes related to parthenolide biosynthesis affected by exogenous application of methyl jasmonate and salicylic acid in Tanacetum parthenium. Plant Cell Rep 34:1909-1918. https://doi.org/10.1007/s00299-015-1837-2
- Martínez Ó, Arjones V, González MV, Rey M (2021) Histone deacetylase inhibitors increase the embryogenic potential and alter the expression of embryogenesis-related and hdac-encoding genes in grapevine (Vitis vinifera 1., Cv. mencía). Plants 10:1164-1183. https://doi.org/10.3390/plants10061164
- Mengel A, Ageeva A, Georgii E, Bernhardt J, Wu K, Durner J, Lindermayr C (2017) Nitric oxide modulates histone acetylation at stress genes by inhibition of histone deacetylases. Plant Physiol 173:1434-1452. https://doi.org/10.1104/pp.16.01734
- Morończyk J, Braszewska A, Wójcikowska B, Chwiałkowska K, Nowak K, Wójcik AM, Kwaśniewski M, Gaj MD (2022) Insights into the histone acetylation-mediated regulation of the transcription factor genes that control the embryogenic transition

- in the somatic cells of Arabidopsis. Cells 11:863. https://doi. org/10.3390/cells11050863
- Nowak K, Wójcikowska B, Gajecka M, Elżbieciak A, Morończyk J, Wójcik AM, Żemła P, Citerne S, Kiwior-Wesołowska A, Zbieszczyk J, Gaj MD (2024) The improvement of the in vitro plant regeneration in barley with the epigenetic modifier of histone acetylation, trichostatin A. J App Gene 65(1):13-30. https://doi. org/10.1007/s13353-023-00800-9
- Pareek A, Suthar M, Rathore GS, Bansal V (2011) Feverfew (Tanacetum parthenium L.): a systematic review. Pharmacogn Rev 5(9):103-110. https://doi.org/10.4103/0973-7847.79105
- Samantara K, Shiv A, de Sousa LL, Sandhu KS, Priyadarshini P, Mohapatra SR (2021) A comprehensive review on epigenetic mechanisms and application of epigenetic modifications for crop improvement. Enviro Experi Bot 188:104479. https://doi. org/10.1016/j.envexpbot.2021.104479
- Sarmiento-López LG, López-Meyer M, Sepúlveda-Jiménez G, Cárdenas L, Rodríguez-Monroy M (2021) Arbuscular mycorrhizal symbiosis in Stevia rebaudiana increases trichome development, flavonoid and phenolic compound accumulation. Biocatal Agric Biotechnol 31:101889–101897. https://doi.org/10.1016/j. bcab.2020.101889
- Seto E, Yoshida M (2014) Erasers of histone acetylation: the histone deacetylase enzymes. Cold Spring Harb Perspect Biol 6(4):a018713. https://doi.org/10.1101/cshperspect.a018713
- Shahbazian MD, Grunstein M (2007) Functions of site-specific histone acetylation and deacetylation. Annu Rev Biochem 76:75-100. https://doi.org/10.1146/annurev.biochem.76.052705.162114
- Shwab EK, Bok JW, Tribus M, Galehr J, Graessle S, Keller NP (2007) Histone deacetylase activity regulates chemical diversity in Aspergillus. Eukar Cell 6(9):1656-1664. https://doi.org/10.1128/
- Simmons CB, Raj SK, Saxena PK (2002) Morphocytological characterization of feverfew, Tanacetum parthenium (L.) Schultz Bip. J Herbs Spices Med Plants 9(1):29-45. https://doi.org/10.1300/ J044v09n01 05
- Song Y, Liu L, Li G, An L, Tian L (2017) Trichostatin A and 5-Aza-2'-Deoxycytidine influence the expression of cold-induced genes in Arabidopsis. Plant Signal Behav 12(11):e1389828. https://doi.org /10.1080/15592324.2017.1389828
- Su LC, Deng B, Liu S, Li LM, Hu B, Zhong YT, Li L (2015) Isolation and characterization of an osmotic stress and ABA induced histone deacetylase in Arachis Hygogaea. Front Plant Sci 6:512. https://doi.org/10.3389/fpls.2015.00512
- Sun K, Zhu G, Hao J, Wang Y, Zhu W (2018) Chemical-epigenetic method to enhance the chemodiversity of the marine algicolous fungus, aspergillus terreus OUCMDZ-2739. Tetrahedron 74(1):83–87. https://doi.org/10.1016/j.tet.2017.11.039
- Tan S, Liu ZP (2015) Natural products as zinc-dependent histone deacetylase inhibitors. ChemMedChem 10(3):441-450. https:// doi.org/10.1002/cmdc.201402460
- Uddenberg D, Valladares S, Abrahamsson M, Sundström JF, Sundås-Larsson A, Von Arnold S (2011) Embryogenic potential and expression of embryogenesis-related genes in conifers are affected by treatment with a histone deacetylase inhibitor. Planta 234:527-539. https://doi.org/10.1186/1753-6561-5-S7-P151
- Valero-Rubira I, Castillo AM, Burrell MÁ, Vallés MP (2023) Microspore embryogenesis induction by mannitol and TSA results in a complex regulation of epigenetic dynamics and gene expression in bread wheat. Front Plant Sci 13:1058421. https://doi. org/10.3389/fpls.2022.1058421
- Venturelli S, Belz RG, Kämper A, Berger A, von Horn K, Wegner A, Böcker A, Zabulon G, Langenecker T, Kohlbacher O, Barneche F (2015) Plants release precursors of histone deacetylase inhibitors to suppress growth of competitors. Plant Cell 27:3175-3189. https://doi.org/10.1105/tpc.15.00585



- Wang Z, Cao H, Chen F, Liu Y (2014) The roles of histone acetylation in seed performance and plant development. Plant Physiol Biochemis 84:125–133. https://doi.org/10.1016/j.plaphy.2014.09.010
- Watson C, Miller DA, Chin-Sinex H, Losch A, Hughes W, Sweeney C, Mendonca MS (2009) Suppression of NF-KB activity by parthenolide induces X-ray sensitivity through inhibition of split-dose repair in TP53 null prostate cancer cells. Radiat Res 171(4):389– 396. https://doi.org/10.1667/RR1394.1
- Williams RB, Henrikson JC, Hoover AR, Lee AE, Cichewicz RH (2008) Epigenetic remodeling of the fungal secondary metabolome. Org Biomol Chem 6(11):1895–1897. https://doi. org/10.1039/b804701d
- Wójcikowska B, Botor M, Morończyk J, Wójcik AM, Nodzyński T, Karcz J, Gaj MD (2018) Trichostatin a triggers an embryogenic transition in Arabidopsis explants via an auxin-related pathway. Front Plant Sci 9:1353. https://doi.org/10.3389/fpls.2018.01353
- Wójcikowska B, Wójcik AM, Gaj MD (2020) Epigenetic regulation of auxin-induced somatic embryogenesis in plants. Int J Mol Sci 21:7. https://doi.org/10.3390/ijms21072307
- Yang F, Zhang L, Li J, Huang J, Wen R, Ma L, Li L (2010) Trichostatin A and 5-azacytidine both cause an increase in global histone H4

- acetylation and a decrease in global DNA and H3K9 methylation during mitosis in maize. BMC Plant Biol 10(1):1–11. https://doi.org/10.1186/1471-2229-10-178
- Yoshida M, Horinouchi S, Beppu T (1995) Trichostatin A and trapoxin: novel chemical probes for the role of histone acetylation in chromatin structure and function. BioEssays 17(5):423–430. https://doi.org/10.1002/bies.950170510
- Zutz C, Gacek A, Sulyok M, Wagner M, Strauss J, Rychli K (2013) Small chemical chromatin effectors alter secondary metabolite production in aspergillus clavatus. Toxins 5(10):1723–1741. https://doi.org/10.3390/toxins5101723

**Publisher's note** Springer Nature remains neutral with regard to jurisdictional claims in published maps and institutional affiliations.

Springer Nature or its licensor (e.g. a society or other partner) holds exclusive rights to this article under a publishing agreement with the author(s) or other rightsholder(s); author self-archiving of the accepted manuscript version of this article is solely governed by the terms of such publishing agreement and applicable law.



#### Terms and Conditions

Springer Nature journal content, brought to you courtesy of Springer Nature Customer Service Center GmbH ("Springer Nature").

Springer Nature supports a reasonable amount of sharing of research papers by authors, subscribers and authorised users ("Users"), for small-scale personal, non-commercial use provided that all copyright, trade and service marks and other proprietary notices are maintained. By accessing, sharing, receiving or otherwise using the Springer Nature journal content you agree to these terms of use ("Terms"). For these purposes, Springer Nature considers academic use (by researchers and students) to be non-commercial.

These Terms are supplementary and will apply in addition to any applicable website terms and conditions, a relevant site licence or a personal subscription. These Terms will prevail over any conflict or ambiguity with regards to the relevant terms, a site licence or a personal subscription (to the extent of the conflict or ambiguity only). For Creative Commons-licensed articles, the terms of the Creative Commons license used will apply.

We collect and use personal data to provide access to the Springer Nature journal content. We may also use these personal data internally within ResearchGate and Springer Nature and as agreed share it, in an anonymised way, for purposes of tracking, analysis and reporting. We will not otherwise disclose your personal data outside the ResearchGate or the Springer Nature group of companies unless we have your permission as detailed in the Privacy Policy.

While Users may use the Springer Nature journal content for small scale, personal non-commercial use, it is important to note that Users may not:

- 1. use such content for the purpose of providing other users with access on a regular or large scale basis or as a means to circumvent access control:
- 2. use such content where to do so would be considered a criminal or statutory offence in any jurisdiction, or gives rise to civil liability, or is otherwise unlawful:
- 3. falsely or misleadingly imply or suggest endorsement, approval, sponsorship, or association unless explicitly agreed to by Springer Nature in writing:
- 4. use bots or other automated methods to access the content or redirect messages
- 5. override any security feature or exclusionary protocol; or
- 6. share the content in order to create substitute for Springer Nature products or services or a systematic database of Springer Nature journal content

In line with the restriction against commercial use, Springer Nature does not permit the creation of a product or service that creates revenue, royalties, rent or income from our content or its inclusion as part of a paid for service or for other commercial gain. Springer Nature journal content cannot be used for inter-library loans and librarians may not upload Springer Nature journal content on a large scale into their, or any other, institutional repository.

These terms of use are reviewed regularly and may be amended at any time. Springer Nature is not obligated to publish any information or content on this website and may remove it or features or functionality at our sole discretion, at any time with or without notice. Springer Nature may revoke this licence to you at any time and remove access to any copies of the Springer Nature journal content which have been saved.

To the fullest extent permitted by law, Springer Nature makes no warranties, representations or guarantees to Users, either express or implied with respect to the Springer nature journal content and all parties disclaim and waive any implied warranties or warranties imposed by law, including merchantability or fitness for any particular purpose.

Please note that these rights do not automatically extend to content, data or other material published by Springer Nature that may be licensed from third parties.

If you would like to use or distribute our Springer Nature journal content to a wider audience or on a regular basis or in any other manner not expressly permitted by these Terms, please contact Springer Nature at

 $\underline{onlineservice@springernature.com}$